Thermal convection in binary fluid mixtures with a weak concentration diffusivity, but strong solutal buoyancy forces

Andrey Ryskin,[1] Hanns Walter Müller,[1,2] and Harald Pleiner[1]

[1]*Max-Planck-Institut für Polymerforschung, D-55021 Mainz, Germany*
[2]*Theoretische Physik, Universität des Saarlandes, D-66041 Saarbrücken, Germany*

Thermal convection in binary liquid mixtures is investigated in the limit where the solutal diffusivity is weak, but the separation ratio is large. Representative examples are colloidal suspensions such as ferrofluids. With a grain size being large on molecular length scales, the particle mobility is extremely small, allowing to disregard the concentration dynamics in most cases. However, this simplification does not hold for thermal convection: Due to the pronounced Soret effect of these materials in combination with a considerable solutal expansion, the resulting solutal buoyancy forces are dominant. Indeed, convective motion is found to set in at Rayleigh numbers well below the critical threshold for single-component liquids. A nonlinear analysis demonstrates that the amplitude quickly saturates in a state of stationary convective motion.

I. INTRODUCTION

Thermal convection in binary mixtures has attracted much research activity in the past (see [1–3] for a review). In comparison to the pure fluid case, the dynamics and the bifurcation scenario are more complicated due to the extra degree of freedom associated with the concentration field; thereby solutal currents are not only driven by concentration gradients, they also occur in response to temperature inhomogeneities. This is denoted as the thermodiffusive or Soret effect. Its influence on the convective buoyancy force is quantified by the dimensionless separation ratio ψ. The sign of ψ indicates whether temperature and solutal-induced density gradients are coaligned (+) or opposed to each other (−). At negative ψ the motionless conductive state experiences an oscillatory instability, saturating in a nonlinear state of traveling waves [3]. On the other hand, at positive ψ the convective instability remains stationary, but the critical Rayleigh number for the onset of convection is dramatically reduced as compared to the pure-fluid reference value $\mathrm{Ra}_c^0 = 1708$. This is a result of the joint action of thermal and solutal buoyancy forces. The present paper is dedicated to the case of positive ψ in colloidal suspensions.

A typical property of binary mixture convection is the formation of concentration boundary layers [4]. This is a consequence of the fact that the concentration diffusivity D_c in mixtures is usually much smaller than the heat diffusivity κ. For molecular binary mixtures the dimensionless Lewis number $L = D_c / \kappa$ adopts typical values between 0.1 and 0.01 [5]. If colloidal suspensions are under consideration, the time scale separation is even more dramatic. In this context magnetocolloids, also known as ferrofluids, are a canonical example. These materials are dispersions of heavy solid ferromagnetic grains suspended in a carrier liquid [6]. With a typical diameter of 10 nm the particles are pretty large on molecular length scales, resulting in an extremely small particle mobility. This feature is reflected by the Lewis numbers as small as $L = 10^{-4}$ [7]. The smallness of L leads to a situation where demixing effects (if any) take place on time

scales far beyond any reasonable observation time. Thus, in those experiments, where thermodiffusion is irrelevant, ferrofluids can safely be treated as single-component fluid systems.

However, ferrofluids are also known to exhibit a very large separation ratio ψ. This observation is due to the pronounced thermodiffusivity of these materials in combination with the fact that the specific weights of the two constituents (magnetite and water/oil) are quite distinct. Following investigations of Blums *et al.* [7], who carried out experiments with a thermodiffusion chamber, ψ can adopt values up to about 100. Recent light scattering investigations of Bacri *et al.* [8], reveal ψ values between around −200 (for ionic ferrofluids) and up to +30 (cyclohexane carrier) at a volume concentration of 10%. Meanwhile the Soret effect in ferrofluids has also been studied under the influence of an external magnetic field [9–11].

A fairly small number of papers deals with convection in ferrofluids. Most of them treat these liquids as single-component fluids, focusing on the extra drive associated with the temperature dependence of the magnetization (pyromagnetic effect) [12–14]. An experimental study with a binary system of ordinary ψ and L values has been reported some time ago [15]. Quite recently Shliomis and Souhar [16] studied the influence of the concentration field on thermal convection in ferrofluids without an external magnetic field. Using linear arguments they predicted a novel kind of relaxation-oscillation convection to appear at Rayleigh numbers below Ra_c^0. Meanwhile, magnetic field related effects have also been investigated in this problem [17].

The purpose of the present consideration is to work out more closely the role of the concentration field. For the sake of concreteness we phrase the discussion in terms of ferrofluids but point out that the results apply equally well to any binary mixture with small L and large positive ψ.

Provided no magnetic field is applied, thermal convection in a perfectly intermixed ferrofluid is usually believed [16] to behave as a single-fluid system. However, our investigation reveals that this is not correct. Rather it is the combination of
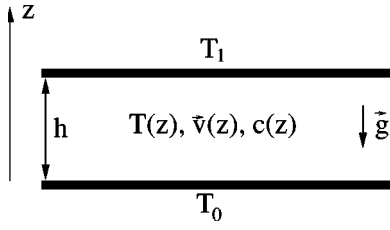
FIG. 1. Sketch of the setup. For details see text.

both, the weak solutal diffusivity and the pronounced solutal buoyancy force, which renders the convective dynamics distinct from the pure-fluid case. It will be demonstrated below that a Rayleigh-Bénard setup will become unstable at Rayleigh numbers well below Ra_c^0. Within a time, small compared to the creeping solutal diffusion time, convective perturbations are found to grow up and saturate in a stationary convective state.

The rest of the paper is organized as follows. In the next section the problem is set up along with the governing equations and boundary conditions. Section III presents a linear analysis specially tailored to account for the slow concentration diffusion. In Sec. IV a Galerkin model is employed for predicting the long time nonlinear convective behavior.

II. SETTING UP THE PROBLEM

Let us consider a laterally infinite horizontal layer of an incompressible ferrofluid (density ρ, kinematic viscosity ν) bounded by two rigid impermeable plates (see Fig. 1). The setup is heated from below with a temperature difference ΔT between the plates. In the present paper we do not consider magnetic field related effects, thus the evolution equations for nonmagnetic binary mixtures can be adopted. Taking $C(\mathbf{r},t)$ as the concentration of the solid constituent of the suspension, the dimensionless equations for the Eulerian fields of velocity $\mathbf{v}(\mathbf{r},t)$, temperature $T(\mathbf{r},t)$, and $C(\mathbf{r},t)$ read in the Boussinesq approximation [18–20]:

$$\mathbf{\nabla}\cdot\mathbf{v}=0, \tag{1}$$

$$\partial_t\mathbf{v}+\mathbf{v}\cdot\mathbf{\nabla}\mathbf{v}=-\mathbf{\nabla}W+\mathrm{Pr}\,\mathbf{\nabla}^2\mathbf{v}$$
$$+\mathrm{Pr}\,\mathrm{Ra}[(T-\bar{T})-\psi(C-\bar{C})]\mathbf{e}_z, \tag{2}$$

$$\partial_t T+\mathbf{v}\cdot\mathbf{\nabla}T=\mathbf{\nabla}^2T, \tag{3}$$

$$\partial_t C+\mathbf{v}\cdot\mathbf{\nabla}C=L(\mathbf{\nabla}^2C+\mathbf{\nabla}^2T). \tag{4}$$

Here, we have scaled length by the layer thickness h, time by the characteristic heat diffusion time h^2/κ, temperature by ΔT, and the concentration by $(D_T/D_c)\Delta T$. The scale for the pressure W is $\kappa^2\rho/h^2$; thereby κ, D_C, D_T are the coefficients for heat, concentration and thermodiffusion, respectively. The quantities $\bar{T}$ and $\bar{C}$ are reference values defined as the mean values for temperature and concentration. Apart from the Prandtl number $\mathrm{Pr}=\nu/\kappa$ and the Lewis number $L=D_c/\kappa$ there is a third dimensionless material parameter, the separation ratio $\psi=D_T\beta_c/(D_c\beta_T)$, where $\beta_T=-(1/\rho)\partial\rho/\partial T$ and $\beta_c=(1/\rho)\partial\rho/\partial c$ are the thermal and

the solutal expansion coefficients, respectively. The dimensionless Rayleigh number $\mathrm{Ra}=\beta_T g h^3\Delta T/(\kappa\nu)$ is the control parameter measuring the strength of the thermal drive. In Eq. (4) we have suppressed the Dufour effect (heat current driven by a concentration gradient), as it is significant in gas mixtures only.

The equations of motion are to be completed by the boundary conditions: Taking the bounding plates to be no slip for the velocity, highly heat conducting, and impermeable for concentration currents we have at the upper ($z=1/2$) and the lower ($z=-1/2$) plates

$$\mathbf{v}|_{z=\pm 1/2}=0, \tag{5}$$

$$T|_{z=\pm 1/2}=\bar{T}\mp\tfrac{1}{2}, \tag{6}$$

$$(\partial_z C+\partial_z T)|_{z=\pm 1/2}=0. \tag{7}$$

Equation (7) guarantees that a concentration current cannot penetrate the plates. Owing to the Soret effect the applied temperature difference enforces a finite concentration gradient at the boundaries. Equations (1)–(4) together with the boundary conditions (5)–(7) complete the system of hydrodynamic equations for the variables $\mathbf{v},T,C$.

III. LINEAR STABILITY ANALYSIS

A. Basic state and time scale separation

It is easy to show that the above boundary-value problem has a simple stationary solution, the so-called conductive state. It is represented by linear temperature and concentration distributions

$$\mathbf{v}=0, \tag{8}$$

$$T_{cond}(z)=\bar{T}-z, \tag{9}$$

$$C_{cond}=\bar{C}+z. \tag{10}$$

In order to check for the stability of this solution one usually proceeds by introducing small perturbations around the conductive state and following their time evolution as governed by the linearized equations of motion. However, owing to the smallness of the Lewis number, the time necessary to establish C_{cond} exceeds the equilibration time for T_{cond} by a factor $1/L$. Take, for instance, a layer with a depth of $h=3$ mm [16]. Then T_{cond} is adopted after a few thermal diffusion times $t_{td}\equiv h^2/\kappa$ ($=1$ in dimensionless units). With the heat diffusivity of water, $\kappa=1.5\times 10^{-7}$ m^2/s, this period amounts to about one minute. On the other hand, for $L=10^{-4}$ the equilibration of the linear concentration profile C_{cond} takes $h^2/(\kappa L)$, i.e., almost a week! Clearly, this tops any reasonable time scale at which convection experiments are carried out. Accordingly, a linear stability analysis, suitable for a comparison with the experiments, has to account for the creeping solutal diffusivity. This can be accomplished by taking the slowly establishing conducting concentration profile $C_0(z,t)$ as the basic state rather than the fully devel-

oped profile C_{cond}. For times larger than the evolution time of the temperature profile, $t > t_{td}$, $C_0(z,t)$ obeys the linear partial differential equation

$$\partial_t C_0 = L \partial_z^2 C_0, \tag{11}$$

with the inhomogeneous boundary condition

$$\partial_z C_0|_{z=\pm 1/2} = 1, \tag{12}$$

resulting from Eq. (9). On the creeping time scale of the evolution of $C_0(z,t)$, $\tau \equiv Lt$, the validity condition of Eqs. (11) and (12) reads $\tau \gtrsim L \simeq 10^{-4}$.

Equations (11) and (12) reflect the evolution of the upcoming conductive concentration profile C_{cond}. However, as outlined at the length above, the system has not enough time to reach this state. At best the Soret driven concentration current is able to pile up thin concentration boundary layers along the plates, the depth δ of which remains small in comparison to the distance between the plates ($\delta \ll 1$). This is somewhat difficult to see from the exact solution of Eqs. (11) and (12):

$$C_0(z,t) = z + \frac{4}{\pi} \sum_{n=0}^{\infty} \frac{(-1)^{n+1}}{(2n+1)^2} \exp[-(2n+1)^2 \pi^2 \tau]$$
$$\times \sin(2n+1)\pi z, \tag{13}$$

since for the small τ's, we are interested here, the sum converges extremely slowly. A better feeling of C_0 can be obtained by the solution of the somewhat simpler problem where the boundary conditions (12) are replaced by $\partial_z C_0|_{z=-1/2} = 1$ and $\partial_z C_0|_{z \gg -1/2} \approx 0$ [16]. The solution of this problem is

$$\partial_z C_0^{(approx)}(z,t) = 1 - \mathrm{erf}\left(\frac{1/2+z}{2\sqrt{\tau}}\right), \tag{14}$$

which, for $\tau \gtrsim 10^{-4}$, describes the development of the boundary layer close to $z = -1/2$ very well. [$\mathrm{erf}(x)$ denotes the error function [21].] As long as each boundary layer does not feel the presence of the opposite one, the superposition of Eq. (14) with the corresponding solution at $z = 1/2$ gives the realistic picture of C_0. We will also corroborate this scenario within the nonlinear calculations below.

B. Linear deviations

To probe the stability of the ground state, deviations are added whose time evolution is investigated. To that end we impose [22]

$$C(\boldsymbol{r},t) = C_0(z,t) + c(\boldsymbol{r},t), \tag{15}$$

$$T(\boldsymbol{r},t) = T_{cond}(z) + \theta(\boldsymbol{r},t), \tag{16}$$

and the velocity field $\boldsymbol{v}(\boldsymbol{r},t)$. Linearizing the equations of motion for the convective perturbations $\boldsymbol{v}$, θ, c yields

$$\partial_t \nabla^2 w = \mathrm{Pr}\,\mathrm{Ra}(\partial_x^2 + \partial_y^2)[\theta - \psi c] + \mathrm{Pr}\nabla^4 w, \tag{17}$$

$$\partial_t \theta - w = \nabla^2 \theta, \tag{18}$$

$$\partial_t c + w \partial_z C_0 = L[\nabla^2 c + \nabla^2 \theta]. \tag{19}$$

Here we have taken twice the curl of the Navier-Stokes equation to derive the equation for the vertical component w of the velocity field.

The boundary conditions read as

$$w|_{z=\pm 1/2} = 0, \tag{20}$$

$$\partial_z w|_{z=\pm 1/2} = 0, \tag{21}$$

$$\theta|_{z=\pm 1/2} = 0, \tag{22}$$

$$(\partial_z c + \partial_z \theta)|_{z=\pm 1/2} = 0. \tag{23}$$

Equations (17)–(19) together with Eqs. (20)–(23) are to be solved for a given C_0.

Since the temporal evolution of the boundary layers takes place on the stretched time scale $1/L$ we consider the profile $C_0(z,\tau)$ as being stationary within the period at which convective perturbations grow up to saturation, i.e., $C_0(z,t) \simeq C_0(z)$. The self-consistency of this assumption has to be checked at the end of the calculations. With this approximation of a stationary C_0 all coefficients in Eqs. (17)–(19) are time independent and solutions in the form $\theta, c, w \propto e^{\lambda t} \cos kx$ can be adopted. This leads to

$$\lambda(\partial_z^2 - k^2)w = -\mathrm{Pr}\,\mathrm{Ra}\,k^2(\theta - \psi c) + \mathrm{Pr}(\partial_z^2 - k^2)^2 w, \tag{24}$$

$$\lambda\theta - w = (\partial_z^2 - k^2)\theta, \tag{25}$$

$$\lambda c + w \partial_z C_0 = L(\partial_z^2 - k^2)(c + \theta). \tag{26}$$

Note that the above ordinary differential system is not autonomous since $C_0(z)$ entails an explicit z dependence. Only in the limiting cases where either $\partial_z C_0 = 1$ (fully developed conductive concentration profile, i.e., $C_0 = C_{cond}$) or $\partial_z C_0 = 0$ (uniform concentration distribution), Eqs. (24)–(26) adopt an autonomous form. These two situations will be discussed, in turn, below.

C. Threshold for a fully developed conductive concentration profile

Although the fully developed conductive profile is of minor significance for the present investigation, let us briefly review [2,3] the situation when $C_0 = C_{cond}$ or equivalently $\partial_z C_0 = 1$ is the ground state. To identify the threshold of the stationary instability, we impose $\lambda = 0$. We obtain $(\partial_z^2 - k^2)\theta = -w$ from Eq. (25) and $(\partial_z^2 - k^2)c \simeq w/L$ from Eq. (26), since $L \ll 1$. This allows to neglect thermal versus solutal buoyancy forces in Eq. (24) leading to

$$L(\partial_z^2 - k^2)^3 c - \psi\,\mathrm{Ra}\,k^2 c = 0, \tag{27}$$

with the boundary conditions

$$\partial_z c|_{z=\pm 1/2} \approx 0, \tag{28}$$

$$(\partial_z^2 - k^2)c|_{z=\pm 1/2} = \partial_z(\partial_z^2 - k^2)c|_{z=\pm 1/2} = 0. \quad (29)$$

The solution of this eigenvalue problem is known [23] to provide a stationary instability with a critical wave number $k = k_c = 0$ at

$$\mathrm{Ra}_c^\infty = 720 \frac{L}{\psi}. \quad (30)$$

Taking $L = 10^{-4}$ and $\psi = 10$ we obtain $\mathrm{Ra}_c^\infty \simeq 10^{-2}$, indicating that the threshold of the Soret driven convection is smaller by a factor of 10^5 as compared to the pure fluid threshold $\mathrm{Ra}_c^0 \simeq 1708$. Note, however, that in order to experimentally verify this drastic onset reduction one has to wait for about a week after any temperature step before the linear conductive concentration profile has fully equilibrated. This case will not be pursued further.

D. Threshold at a uniform concentration distribution

We now turn to the opposite limit when the concentration boundary layer had no time to develop, thus $C_0 = \bar{C}$ or, equivalently, $\partial_z C_0 = 0$. Imposing again zero growth rate $\lambda = 0$ we obtain from Eqs. (23) and (26) the equality $c = \theta$. Substituting this into Eq. (24) yields

$$(\partial_z^2 - k^2)^2 w - \mathrm{Ra}\, k^2(1+\psi)\theta = 0, \quad (31)$$

$$(\partial_z^2 - k^2)\theta + w = 0. \quad (32)$$

In combination with the boundary conditions (20) and (22), we recover the known boundary value problem for pure-fluid thermogravitational convection; however, with an extra prefactor $(1+\psi)$ in front of the Rayleigh number. Taking this renormalization into account, and following Chandrasekhar's solution [24], yields an exchange of stability at

$$\mathrm{Ra}_c = \frac{1}{1+\psi}\mathrm{Ra}_c^0 \quad (33)$$

with a critical wave number $k_c = 3.117$ and $\mathrm{Ra}_c^0 \simeq 1708$.

The appreciable value of the separation ratio ψ implies a significant onset reduction. Strictly speaking, the determination of Ra_c by imposing zero growth rate $\lambda = 0$ is void, since the creeping diffusion of C_0 can only be disregarded for times $t \ll L^{-1}$. In other words, the exponential amplification of the *convective* perturbation c has to proceed much faster than the *diffusive* evolution of C_0. This is always true for Rayleigh numbers sufficiently off from Ra_c, i.e., when λ is nonzero with $|\lambda(\mathrm{Ra})| \gg L$. It is this inequality that guarantees the validity of the time scale separation. And it is also the experimentally relevant case because extreme waiting times are circumvented. This situation will be focused on in the following.

E. Linear growth rate

The preceding discussion reveals that a linear stability theory, suitable to compare with a convection experiment, has to rely on the growth rates of the convective perturba-

tions rather than the threshold value. To that end we assume that the spatial profiles of velocity and temperature are only slightly disturbed by the concentration dynamics. Accordingly we represent their dependencies in terms of simple trigonometric test functions in the form

$$w(x,z,t) = A(t)\cos(kx)\cos^2(\pi z), \quad (34)$$

$$\theta(x,z,t) = B(t)\cos(kx)\cos(\pi z). \quad (35)$$

In contrast, for the convective concentration field c we allow for a steep boundary layer behavior, which we account for by the following multimode expansion:

$$c(x,z,t) = -\theta(x,z,t) + \cos(kx)\sum_{n=0}^{n=\infty} b_n(t)\cos(2\pi nz). \quad (36)$$

Again we assume that the conductive concentration boundary layers had not enough time to pile up, thus imposing $\partial_z C_0 = 0$. It is easy to see that Eq. (36) satisfies the boundary conditions (7). Furthermore, it conserves the mirror symmetry of c with respect to the midplane between the boundaries ($z \to -z$). Substituting Eq. (36) into Eqs. (17)–(19), and projecting the equations with the respective Galerkin modes, reveals that only the first two concentration modes b_0 and b_1 enter the evolution equation for A. The remaining concentration modes b_i with $i \geq 2$ are decoupled. Summarizing the Galerkin model for the relevant modes $A(t)$, $B(t)$, $b_0(t)$, $b_1(t)$ leads to the following system of equations:

$$\frac{3k^2 + 4\pi^2}{8\mathrm{Pr}}\lambda A + \left(\frac{3k^4}{8} + k^2\pi^2 + 2\pi^4\right)A$$

$$- \frac{4k^2}{3\pi}\mathrm{Ra}(1+\psi)B + \frac{\psi k^2}{4}\mathrm{Ra}(2b_0 + b_1) = 0, \quad (37)$$

$$\frac{4}{3\pi}\lambda B + \frac{4}{3\pi}(\pi^2 + k^2)B - \frac{3}{8}A = 0, \quad (38)$$

$$\lambda b_0 + Lk^2 b_0 + \frac{2(\pi^2 + k^2)}{\pi}B - \frac{9}{16}A = 0, \quad (39)$$

$$\lambda b_1 + L(k^2 + 4\pi^2)b_1 + \frac{4}{3\pi}(\pi^2 + k^2)B - \frac{3}{8}A = 0. \quad (40)$$

To check the reliability of the above 4-mode approximation, we solved the linearized boundary value problem of Eqs. (17)–(23), exactly by means of the numerical method outlined in Ref. [25]. Comparing the results for the growth rate λ we found that the Galerkin technique is accurate by about 10%.

For $\lambda \gg L$ and $\psi \gg 1$ (with the approximation $k \approx \pi$) an analytical expression for λ as an implicit function of the material and the control parameters (ψ, L, Pr, and Ra, respectively) can be obtained from Eqs. (37)–(40):

$$3\,\mathrm{Ra}\,\mathrm{Pr}(\lambda + 2\pi^2 L\psi) = \lambda(2\pi^2 + \lambda)(27\pi^2\mathrm{Pr} + 7\lambda). \quad (41)$$
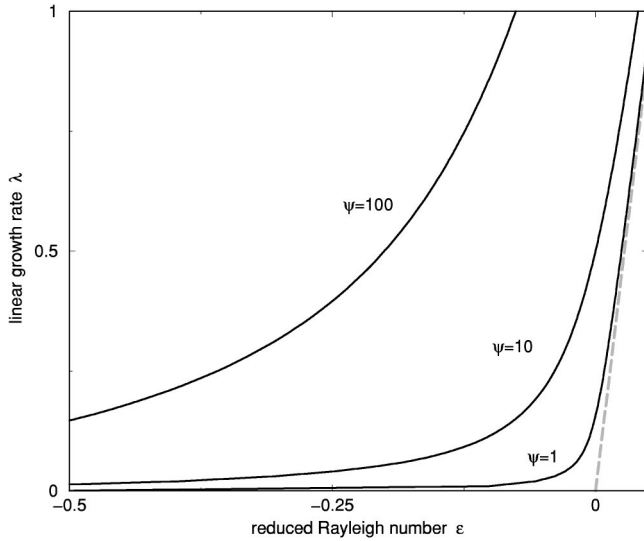
FIG. 2. The linear growth rate $\lambda(\varepsilon)$ for convective perturbations as a function of the reduced Rayleigh number $\varepsilon = \mathrm{Ra}/\mathrm{Ra}_c^0 - 1$. Here Ra_c^0 is the threshold for the onset of convection in a single-component fluid. Within the present Galerkin approximation $\mathrm{Ra}_c^0 = 1752$.

Without these approximations numerical results in Fig. 2 illustrate the dependence of λ on the reduced Rayleigh number $\varepsilon = \mathrm{Ra}/\mathrm{Ra}_c^0 - 1$ for different values of the separation ratio. The dashed line bifurcating at $\varepsilon = 0$ indicates the reference case of single-fluid convection. From Eq. (41) and Fig. 2 it becomes clear that λ depends for large ψ on the product ψL rather than L alone. Thus decreasing the concentration diffusivity L makes the curve $\lambda(\varepsilon)$ approach to the pure fluid case. On the other hand, increasing the solutal buoyancy force by rising ψ has the opposite effect. Assuming that the experimental observation time is long enough to detect an unstable convective mode with a growth rate $\lambda \simeq 0.1$ (i.e., waiting time of about 10 heat diffusions times, which in a layer of thickness $h = 3$ mm corresponds to about 10 min and which is still much shorter than L^{-1}, the time scale of C_0), then convective motion is detectable at Rayleigh numbers 10–50 % below Ra_c^0 depending on the value ψ.

To corroborate the validity of the time scale separation we have also solved the linear problem, where the approximative uniform concentration distribution $\partial_z C_0 = 0$ was replaced by the true profile, as given by Eq. (14) at $t = 10$. Reevaluating the growth rate yields a value for λ, which differs from the previous one by less than 10 %.

Regarding typical ψ values in the range $\psi \simeq 10$–100, Eq. (33) indicates that the convective onset threshold Ra_c for a homogeneously intermixed ferrofluid experiences a significant reduction relative to the pure-fluid value Ra_c^0 (cf. Sec. III D). This result appears somewhat counterintuitive: As long as the initial concentration profile is approximately uniform, one might expect convection to behave as in single-component liquids [16]. But it turns out here that this argument is not generally applicable, provided the applied Rayleigh number is not too far below the reference value Ra_c^0, Fig. 2 reveals that the *conductive* profile $C_0(z,\tau)$ and

the *convective* one $c(\mathbf{r},t)$ evolve on strongly distinct time scales. While the former always proceeds on the creeping time scale $1/L$, the quantity $c(\mathbf{r},t)$ grows up much more rapidly proportional to $e^{\lambda t}$, in unison with θ and w. Then, owing to the pronounced ψ value, solutal buoyancy forces significantly contribute to the destabilization of the conductive state.

Our observations shed light on a state of relaxation-oscillation convection predicted recently by Shliomis and Souhar [16]. In that paper it was argued that after a sudden application of $\mathrm{Ra} < \mathrm{Ra}_c^0$ to a ferrofluid with an initial uniform concentration distribution, a concentration boundary layer along the plates piles up slowly, making the instantaneous convective threshold $\mathrm{Ra}_c(t)$ gradually sink below the applied Ra value. Then the increasing convective motion mixes up the ferrofluid, sweeping out the concentration boundary layers. With the concentration profile being rehomogenized, the ferrofluid was argued to behave like a single-component liquid, returning to the conductive state since the applied Rayleigh number is smaller than Ra_c^0. Thereafter this relaxation-oscillation cycle can start again. The present investigation reveals that such a cycle cannot work: This is because it was proven that convective perturbations in a homogeneously mixed ferrofluid do not decay at $\mathrm{Ra}_c < \mathrm{Ra} < \mathrm{Ra}_c^0$. Rather they may experience a considerable positive growth rate (see Fig. 2) even at Rayleigh numbers 50% below Ra_c^0, say. We conclude that there is no mechanism, that drives the system back to the conductive state. Once initiated, convection will persist (rather than oscillate) and saturate in a stationary nonlinear state. This will be shown in the following section.

IV. NONLINEAR BEHAVIOR

The preceding linear analysis reveals that for Rayleigh numbers well below Ra_c^0, convective fluctuations are exponentially amplified on a time scale, which is experimentally relevant. It can therefore be expected that these fluctuations saturate quickly in a nonlinear convective pattern. To work out whether this final state is stationary or oscillatory we solved the nonlinear problem by use of numerical methods. To that end we make the following ansatz of a two-dimensional pattern, which is laterally (in x direction) periodic with wave number k:

$$C(x,z,t) = C_0(z,t) + c(x,z,t) = C_0(z,t) + c_1(z,t)\cos kx, \tag{42}$$

$$T(x,z,t) = -z + \theta(x,z,t) = \theta_0(z,t) + \theta_1(z,t)\cos kx, \tag{43}$$

$$v_x(x,z,t) = -(1/k)\partial_z w_1(z,t)\sin kx, \tag{44}$$

$$v_z(x,z,t) = w_1(z,t)\cos kx, \tag{45}$$

with incompressibility already built in. Substituting Eqs. (42)–(45) into the nonlinear equations of motion (2)–(4) and sorting for different lateral dependences yield the following system of equations:

$$\frac{1}{\text{Pr}}\partial_t(\partial_z^2-k^2)w_1=(D^2-k^2)^2w_1-\text{Ra}\,k^2(\theta_1-\psi c_1),$$

$$(46)$$

$$\partial_t C_0+\frac{1}{2}\partial_z(w_1c_1)=L\partial_z^2(C_0+\theta_0),\qquad(47)$$

$$\partial_t c_1+w_1\partial_z C_0=L(\partial_z^2-k^2)(c_1+\theta_1),\qquad(48)$$

$$\partial_t\theta_0+\frac{1}{2}\partial_z(w_1\theta_1)=\partial_z^2\theta_0,\qquad(49)$$

$$\partial_t\theta_1-w_1+w_1\partial_z\theta_0=(\partial_z^2-k^2)\theta_1,\qquad(50)$$

with the boundary conditions

$$\partial_z(c_1+\theta_1)|_{z=\pm1/2}=0,\qquad(51)$$

$$\partial_z(C_0+\theta_0)|_{z=\pm1/2}=1,\qquad(52)$$

$$\theta_1|_{z=\pm1/2}=\theta_0|_{z=\pm1/2}=0,\qquad(53)$$

$$w_1|_{z=\pm1/2}=\partial_z w_1|_{z=\pm1/2}=0.\qquad(54)$$

To solve this boundary-value problem we adopt vertical profiles w_1, θ_0, θ_1, C_0, and c_1 in the form

$$w_1(z,t)=A(t)\cos^2(\pi z),\qquad(55)$$

$$\theta_1(z,t)=B(t)\cos\pi z,\qquad(56)$$

$$\theta_0(z,t)=F(t)\sin2\pi z,\qquad(57)$$

$$C_0(z,t)=z-\theta_0(z,t)+\sum_{n=0}^{n=N}a_n(t)\sin(2n+1)\pi z,\quad(58)$$

$$c_1(z,t)=-\theta_1(z,t)+\sum_{n=0}^{n=N}b_n(t)\cos2n\pi z,\qquad(59)$$

which satisfy the boundary conditions (51)–(54) identically. The above equations describe two-dimensional convection in the form of parallel rolls along the y axis in an infinite slab of thickness 1. We point out that for $\psi=0$, the concentration fields decouple from temperature and velocity. This reduces Eqs. (55)–(57) to the 3-mode model introduced by Lorenz [26] to mimic the dynamics of convective rolls in single-component Rayleigh-Bénard convection. At nonzero ψ, convection is modified by the concentration field but we can adopt the above few-mode expansions for temperature and velocity without modifications, because the diffusivities for heat and momentum are large enough to prevent the appearance of strong gradients. By way of contrast, owing to the small Lewis number, the concentration field does build up steep boundary layers, which we account for by multimode Fourier series as given in Eqs. (58) and (59). For C_0 the modes are antisymmetric in z and resemble the solution (13), while for c_1 symmetric modes are appropriate. The number N of contributing modes was taken large enough to ensure that the results are insensitive against a further increase of N. For the parameter values considered here, $N=20$ turned out to be sufficient.

The equations for the mode amplitudes A,B,F,a_n,b_n have been solved by a Runge-Kutta integration. The wave number k, usually taken to be the mode of maximum linear growth rate $\lambda(k,\text{Ra})$ varies between 3 and 3.5 within the investigated Rayleigh number regime. However, since the final predictions of our model turned out not to depend sensitively on the k value chosen we adopted in all of our simulations $k=\pi$. All runs were started from an initial configuration characterized by a undisturbed linear temperature profile $T=T_{cond}$, a uniform concentration distribution $\partial_z C_0=c_1=0$, and small random velocity fluctuations. The time evolution of the velocity amplitude $A(t)$ as obtained from a typical simulation run is presented in Fig. 3 for two different values of the Rayleigh number ($\varepsilon=\text{Ra}/\text{Ra}_c^0-1=\pm5.7\%$) on either side of the pure-fluid reference threshold Ra_c^0. The dashed line in Fig. 3 denotes pure-fluid reference case $\psi=0$. In all of our runs the convective motion was found to settle in a state of *stationary* convection. A relaxation oscillation behavior as predicted in Ref. [16] could not be observed. The times necessary to reach the saturation values are several thermal diffusion times and increase with decreasing ε. However, they are still much shorter than the evolution time of the creeping concentration profile, thus corroborating our assumption $\partial_z C_0=0$ in the preceding section. The overshoot in Fig. 3 before the plateau values are reached is not a numerical artifact, but it may be related to the small number of lateral modes we have taken into account. This can be expected, since additional modes with negative growth rate smooth out the relaxation into the saturated state.

Figure 4 shows the corresponding bifurcation diagram with the dependence of the saturation amplitude on the reduced Rayleigh number. At $\varepsilon>0$ the amplitude saturates at a value that does not significantly deviate from the single-component case. On the other hand, the influence of the concentration field is most pronounced for $\text{Ra}\lesssim\text{Ra}_c^0$. This is a consequence of the competitive interaction between the
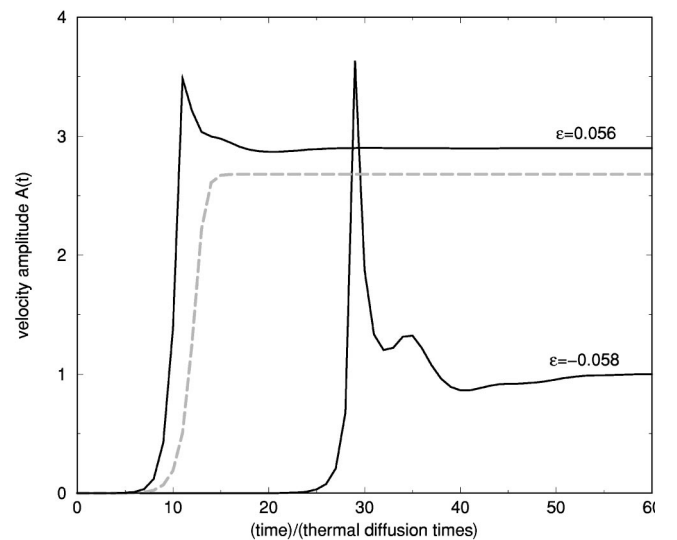
FIG. 3. The time dependence of the velocity amplitude $A(t)$ for positive and negative values of $\varepsilon=\text{Ra}/\text{Ra}_c^0-1$ in terms of the thermal diffusion time t_{td} (for $\text{Pr}=7$ and $L=7\times10^{-5}$). The dashed gray line corresponds to single-component fluid ($\psi=0$) $\varepsilon=0.056$.
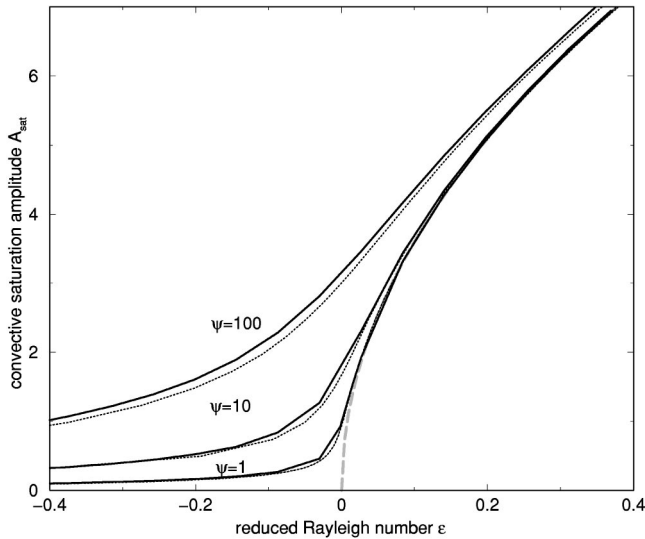
FIG. 4. The saturation amplitude $A_{sat}=A(t\rightarrow\infty)$ as a function $\varepsilon=\mathrm{Ra}/\mathrm{Ra}_c^0-1$ (parameters as in Fig. 3). The dashed gray line corresponds to a single-component fluid ($\psi=0$). Dotted lines show the result of a 7-mode Galerkin approximation as given by Eq. (4.1b) in Ref. [22].

small Lewis number and the large separation ratio. Decreasing L makes the curve in Fig. 4 approach to the dashed reference line, whereas rising ψ has the opposite effect as it amplifies the solutal buoyancy forces. For the sake of comparison the dotted lines in Fig. 4 show an analytical approximation for the saturated velocity amplitude based on a 7-mode Galerkin approximation recently introduced by Hollinger, Lücke, and Müller [Eq. (4.1b) in Ref. [22]].

Unlike a single-component system, where convective perturbations decay for negative ε, the ferrofluid exhibits a pronounced positive linear growth rate (cf. Fig. 2). When measuring a bifurcation diagram such as Fig. 4, one might conclude that the bifurcation is imperfect. Indeed, a slight imperfect behavior was observed in the experiments of Bigazzi, Ciliberto, and Croquette [15] and of Schwab, Hildebrandt, and Stierstadt [14], who recorded the convective heat transport as a function of Ra. But we learn here that this phenomenon is to be attributed to the concentration dynamics: As outlined in Sec. 3, the very onset for convection is located at a much smaller Rayleigh number Ra_c, but at Rayleigh numbers slightly larger the linear growth rate of disturbances remains extremely small. Thus, trying to detect Ra_c in such an experiment would be hopeless, as it requires extremely long observation times. Experiments on ferrofluids have been reported recently [27] that corroborate the behavior shown in Fig. 4.

In contrast, at ε around ±10–20% the time necessary to wait for the equilibration of the nonlinear convective state amounts to only a few *thermal* diffusion times (see Fig. 3). This statement, which holds in particular also for the concentration field, demonstrates that the growth of convective perturbations is a fast process on the (creeping) time scale $1/L$ of solutal diffusion. On the first view this might appear counterintuitive, but it can be seen from Fig. 5 that the final concentration distribution differs from the initial homoge-
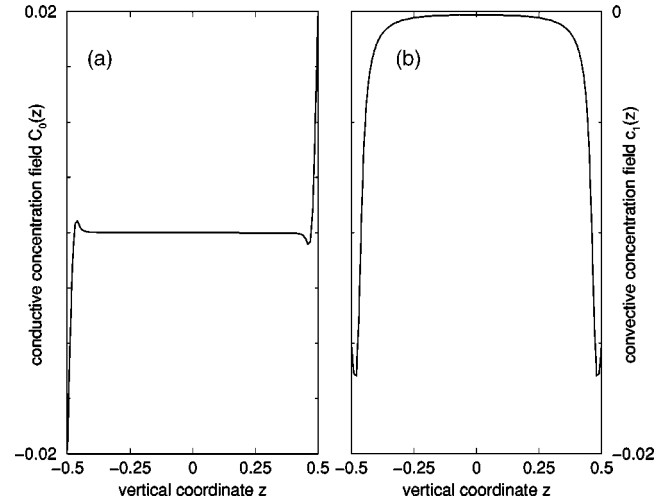
FIG. 5. (a) The conductive concentration profile $C_0(z)=C_0(z,t\rightarrow\infty)$ in the fully developed saturated state for $\varepsilon=-0.058$ (parameters $\mathrm{Pr}=7$, $L=7\times10^{-5}$, and $\psi=10$). (b) Same as (a) for the convective concentration field $c_1(z)=c_1(z,t\rightarrow\infty)$.

neous profile only in *thin* boundary layers. Consequently, time consuming redistribution processes of the concentration field are not necessary for building up the solutal saturation profiles. This keeps the equilibration time small and no further evolution on the slow diffusion time scale occurs after the system reaches the state given in Fig. 5.

V. CONCLUSION

Thermoconvection of binary mixtures with a weak concentration diffusivity and a large separation number has been investigated theoretically. By considering the classical Rayleigh Bénard setup, it is shown that both the linear as well as the nonlinear convective behavior is significantly altered by the concentration field as compared to single-component systems. Starting from an initial motionless configuration with a uniform concentration distribution, convective perturbations are found to grow even at Rayleigh numbers well below the threshold Ra_c^0 of pure-fluid convection. It turned out that the actual critical Rayleigh number Ra_c is drastically smaller, but experimentally inaccessible due to the extremely slow growth of convection patterns for $\mathrm{Ra}\gtrsim\mathrm{Ra}_c$, requiring extremely large observation times. On the other hand, operating the ferrofluid convection experiment at Rayleigh numbers $\mathrm{Ra}_c<\mathrm{Ra}\lesssim\mathrm{Ra}_c^0$, reveals considerable positive growth rates, which lead to a saturated nonlinear state almost as fast as pure-fluid convection does at $\mathrm{Ra}>\mathrm{Ra}_c^0$. This result is corroborated by earlier convection experiments. It does not comply with a recent prediction of convective self-oscillations conjectured from the interplay between short thermal and slow solutal diffusion time scales.

[1] J.K. Platten and J.C. Legros, *Convection in Liquids* (Springer, Berlin, 1984).

[2] M.C. Cross and P.C. Hohenberg, Rev. Mod. Phys. **49**, 581 (1993).

[3] M. Lücke, W. Barten, P. Büchel, C. Fütterer, St. Hollinger, and Ch. Jung, in *Pattern Formation in Binary Fluid Convection and in System with Throughflow*, edited by F.H. Busse and S.C. Müller, Lecture Notes in Physics Vol. 55 (Springer, Berlin, 1998), p. 127.

[4] B. Huke, M. Lücke, P. Büchel, and Ch. Jung, J. Fluid Mech. **408**, 121 (2000).

[5] P. Kolodner, H. Williams, and C. Mac, J. Chem. Phys. **88**, 6512 (1988).

[6] R.E. Rosensweig, *Ferrohydrodynamics* (Cambridge University Press, Cambridge, 1985).

[7] E. Blums, A. Mezulis, M. Maiorov, and G. Kronkalns, J. Magn. Magn. Mater. **169**, 220 (1997).

[8] J. Lenglet, A. Bourdon, J.-C. Bacri, and G. Demouchy (unpublished).

[9] E. Blums, S. Odenbach, A. Mezulis, and M. Maiorov, J. Magn. Magn. Mater. **201**, 268 (1999).

[10] E. Blums, J. Magn. Magn. Mater. **149**, 111 (1995).

[11] S. Odenbach, J. Magn. Magn. Mater. **149**, 116 (1995).

[12] B.A. Finlayson, J. Fluid Mech. **40**, 753 (1970).

[13] A. Recktenwald and M. Lücke, J. Magn. Magn. Mater. **188**, 326 (1998).

[14] L. Schwab, U. Hildebrandt, and K. Stierstadt, J. Magn. Magn. Mater. **39**, 113 (1983); L. Schwab, Ph.D. thesis, Munich, 1989.

[15] P. Bigazzi, S. Ciliberto, and V. Croquette, J. Phys. (France) **51**, 611 (1990).

[16] M.I. Shliomis and M. Souhar, Europhys. Lett. **49**, 55 (2000).

[17] M.I. Shliomis and B. Smorodin, J. Magn. Magn. Mater. **252**, 197 (2002).

[18] J. Boussinesq, *Théorie Analytique de la Chaleur* (Gauthier-Villars, Paris, 1903), Vol. II, p. 172.

[19] J.K. Platten and G. Chavepeyer, Int. J. Heat Mass Transf. **19**, 27 (1976).

[20] H.R. Brand, P.C. Hohenberg, and V. Steinberg, Phys. Rev. A **30**, 2548 (1984).

[21] A. Abramowitz and I.A. Stegun, *Handbook of Mathematical Functions* (Dover Publications, New York, 1965).

[22] S. Hollinger, M. Lücke, and H.W. Müller, Phys. Rev. E **57**, 4250 (1998).

[23] D.T.J. Hurle, E. Jackeman, and E.R. Pike, Proc. R. Soc. London, Ser. A **296**, 469 (1967).

[24] S. Chandrasekhar, *Hydrodynamic and Hydromagnetic Stability* (Clarendon Press, Oxford, 1961).

[25] N. Li, J.O. Murphy, and J.M. Steiner, Z. Angew. Math. Mech. **75**, 3 (1995).

[26] E.N. Lorenz, J. Atmos. Sci. **20**, 130 (1963).

[27] S. Odenbach (private communication).